Aerospace Science and Technology 107 (2020) 106238

Contents lists available at ScienceDirect

Aerospace Science and Technology

www.elsevier.com/locate/aescte

A novel concept of VTOL bi-rotor UAV based on moving mass control

Shahin Darvishpoor *, Jafar Roshanian, Morteza Tayefi

Faculty of Aerospace Engineering, K.N. Toosi University of Technology, Tehran, Iran

ARTICLE INFO

Article history:
Received 9 January 2020
Received in revised form 23 May 2020
Accepted 22 September 2020
Available online 25 September 2020
Communicated by Christian Circi

Keywords:
Moving mass control
UAV
VTOL
Mathematical modeling
Control

ABSTRACT

This paper presents a novel concept of a co-axial bi-rotor UAV which is controlled by moving its center of gravity. After deriving a 6DOF nonlinear model using the Euler-Newton method, we introduce a simplified 3DOF model for planar motion. Due to the limited available torque in pitch and roll channels, a linear quadratic regulator controller is designed for planar motion control, in order to evaluate the performance and maneuverability of the system while respecting the control limits. The simulation results of implementing an LQR controller on the nonlinear model for tracking problem shows that the system has convincing performance, and while control inputs are constrained, controlling the system is possible with no significant restrictions. Even with considering a first-order dynamic for the actuators, the implementation of the LQR controller for tracking an 8-shape trajectory considering different uncertainties shows that the system has high enough maneuverability for a wide range of applications, like Air Shipping and Delivery, Photography and Multimedia, Monitoring (Traffic, Wildlife, Industry, ...), Search and Rescue, Weather Forecasting, etc.

1. Introduction

In recent years, drones have been used in a variety of fields, from agriculture, forestry, multimedia to transportation [1], traffic monitoring [2], remote sensing [3] and other civilian applications [4], each of these applications have their own specific needs, like long endurance, low energy consumption, high maneuverability, high stability and so on. It is hardly possible to gather all of those benefits in an Unmanned Aerial Vehicle (UAV) at the same time, this has led to the development of various types of drones from Vertical Takeoff and Landing (VTOL) and Horizontal Takeoff and Landing (HTOL) to Hybrid and Bio-Inspired UAVs [5].

Throughout most of this history, VTOL UAVs especially multi-rotors, have been mainly the focal point of researchers' attention, specifically because of their simplicity, low cost, no need for a runway to takeoff or landing and capability of being used in various applications [6]. Researchers have used a range of ideas to design and build these types of UAVs including tilt-rotors, ducted fans, semi-flapping rotors, thrust vectoring, embedded fans and Dyson fans [5], [7] one of the ideas which recently is used in multirotors is moving the center of gravity to control the UAV.

Moving Mass Control (MMC) is a control mechanism that uses internal moving masses to adjust the center of gravity and thereby control the attitude. While this type of control has been mostly used in underwater vehicles, there are applications of this method in the aerospace industry, e.g. re-entry vehicles, spacecrafts, satellites, and UAVs, a comprehensive review paper is published by Li et al. on the applications of MMC [8]. Particularly in re-entry vehicles, MMC has various applications [9], for example, Dong and his colleagues used MMC to control the roll channel of a re-entry vehicle with considerations of full state constraints [10], another work has been done for increasing the stability of a re-entry vehicle by Mohammadi [11]. Many control methods like adaptive control [12], sliding mode control [13], different kinds of optimal controls and also controllers which are designed in combination with modern methods like machine learning, are implemented on Moving Mass (MM) systems [8].

In multirotors there are few researches about using MMC as a control mechanism, the first try of using MMC in multirotors comes back to 2008 when Bermes et al. Developed their new design of steering mechanism for a mini coaxial helicopter, in their concept they used a MM mechanism as an alternative for swash plate steering [14]. Yadav et al. also developed a similar MAV using COG shifting mechanism [15]. Haus and his colleagues also came up with the idea of using MMC in quadrotors, they developed an experimental model of a quadrotor with MMC mechanism using four miniature two-stroke combustion engines to supply the required lift force and four moving masses to control the attitude of the quadrotor [16].

Compared to other control methods such as using control surfaces, MMC has two major advantages:

* Corresponding author.
E-mail address: darvishpoor@email.kntu.ac.ir (S. Darvishpoor).

https://doi.org/10.1016/j.ast.2020.106238
1270-9638/

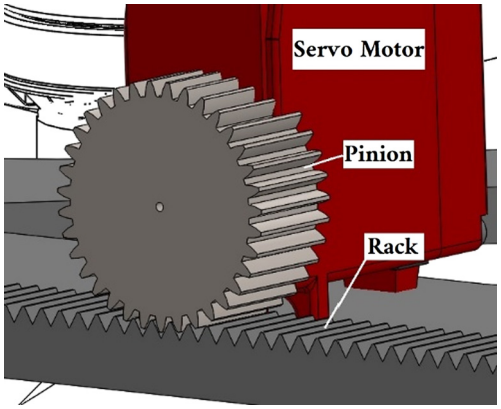

Fig. 1. The rack and pinion mechanism used to move the masses.

1. Mechanisms and actuators are completely inside the body and hence have no aerodynamic effect.

2. Since there is no need to use a fraction of the aerodynamic forces to control the system, maximum use of aerodynamic forces will be provided, resulting in lower energy consumption and greater payload capacity specially in cruise flight [8].

Comparing with other works specifically with comparison to re-entry vehicles, using MMC as a control method in multirotors have another advantage, in this method we take advantage of MMC not only for providing stability but also for controlling purposes. This concept also enables us to compensate for mass imbalances caused by low accuracy during the manufacturing process.

Contrary to other MMC UAVs, for example Haus's concept, which uses four rotors in the structure of a quadrotor, we only use two rotors and in a new structure, we place the moving masses on sides of the main frame, this novel configuration increases the maximum available shift of COG and as a result the maximum available torques this is what increases the maneuverability of the system, and reduces the overall mass and cost. Furthermore in spite of Bermes's co-axial helicopter this structure is more suitable to carry cargo meanwhile it uses two separate rotors instead of one contra-rotating rotor, which allows us to control the yaw channel when it is needed, furthermore this configuration allows us to put the batteries and other equipment inside the body. Also, the MM mechanisms are completely different, while Bermes uses a spherical MM mechanism with two swings we use a simple rack an pinion linear MM mechanism. As shown in following sections, this novel configuration of a moving mass controlled UAV has a high maneuverability and is suitable for a vast field of applications.

2. Concept description

The main idea in this paper is to control the attitude of the UAV by controlling the Center of Gravity (CoG). This can be reached by using four moving masses. In our concept, we use two co-axial rotors which are rotating in the opposite direction of each other, at the center of a square frame and four moving masses on four sides of the frame according to Fig. 2.

We use a pair of Clockwise (CW) and Counter Clockwise (CCW) propellers, in order to eliminate reaction torques produces by each rotor (and propeller).

There are different mechanisms for moving the masses, including reels, rails, straps, and gears, in this concept we use rack and pinion mechanism which is controlled by a servo motor. This mechanism is fast enough, inexpensive and easy to run, and we can consider its dynamics as a first-order system (see Fig. 1).

The yaw angle is controlled by creating a differential angular velocity of $\Delta\omega$ between two rotors, and only roll and pitch angles are controlled by moving the CoG. By moving the masses in X, Y direction, the lift force of two rotors will produce a torque about CoG which causes the UAV to rotate and enables us to control the UAV.

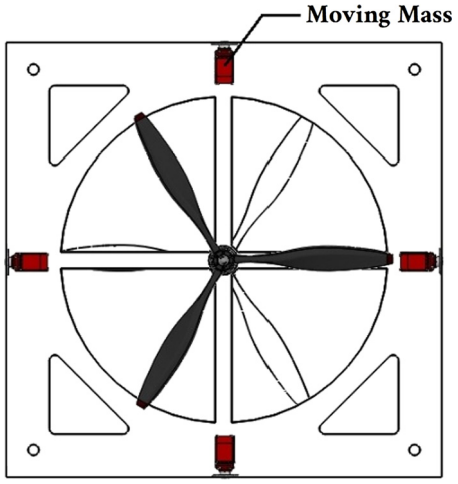

Fig. 2. Schematic of moving CoG bi-rotor VTOL UAV concept.

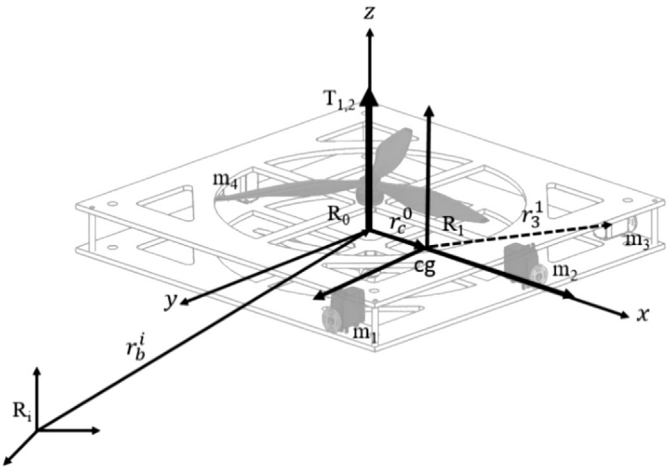

Fig. 3. Reference frames.

3. Mathematical modeling

First of all, we should explain the reference frames which are used in this section. We use three different reference frames, Earth Fixed Inertial Frame, Rotating Body Frame, and Rotating CoG frame.

We consider the Earth Fixed Inertial Frame (R_i) as a fixed frame at a desired origin. Body Frame (R_0) is considered as a Body-Fixed frame at the center of surface, and finally, one more frame is considered which is parallel to the body frame at CoG, we will show this frame by R_1 (see Fig. 3).

For any desired vector in any frame, we use r_a^b notation which shows a vector from the origin to the object a in reference frame b.

We use ZYX Euler angles to represent the orientation of the UAV in the R_i frame Thus the transformation matrix of position from the body frame to the vertical inertial frame will be [17]:

$$T_b^v = R_x(\varphi)\, R_y(\theta)\, R_z(\psi) \tag{1}$$

where:

$$R_x(\varphi) = \begin{bmatrix} 1 & 0 & 0 \\ 0 & c(\varphi) & -s(\varphi) \\ 0 & s(\varphi) & c(\varphi) \end{bmatrix} \tag{2}$$

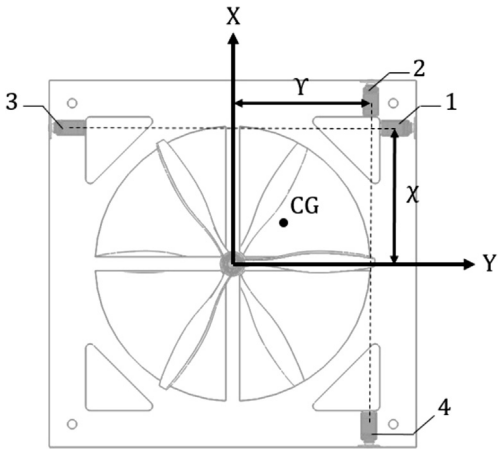

Fig. 4. General displacement of the moving masses.

$$R_y(\theta) = \begin{bmatrix} c(\theta) & 0 & s(\theta) \\ 0 & 1 & 0 \\ -s(\theta) & 0 & c(\theta) \end{bmatrix} \tag{3}$$

$$R_z(\psi) = \begin{bmatrix} c(\psi) & -s(\psi) & 0 \\ s(\psi) & c(\psi) & 0 \\ 0 & 0 & 1 \end{bmatrix} \tag{4}$$

where c and s denote *cos* and *sin* respectively. Similarly, for angular velocity transformation matrix we have [18]:

$$T_{bv} = \begin{bmatrix} 1 & s(\varphi)t(\theta) & c(\varphi)t(\theta) \\ 0 & c(\varphi) & -s(\varphi) \\ 0 & \frac{s(\varphi)}{c(\theta)} & \frac{c(\varphi)}{c(\theta)} \end{bmatrix} \tag{5}$$

where t denotes tan. So, if we define angular and linear velocities of the UAV in the body frame as:

$$\omega_b = \begin{Bmatrix} p \\ q \\ r \end{Bmatrix} \quad V_b = \begin{Bmatrix} u \\ v \\ w \end{Bmatrix} \tag{6}$$

Then the angular and linear velocities in the inertial frame can be calculated like this [18]:

$$\omega = T_{bv}\omega_b \tag{7}$$

$$V = T_{bv}V_b \tag{8}$$

so, the kinematic equations are:

$$\begin{aligned} \dot{\varphi} &= p + r(\cos(\varphi)\tan(\theta)) + q(\sin(\varphi)\tan(\theta)) \\ \dot{\theta} &= q(\cos(\varphi)) - r(\sin(\varphi)) \\ \dot{\psi} &= r\left(\frac{\cos(\varphi)}{\cos(\theta)}\right) + p\left(\frac{\sin(\varphi)}{\cos(\theta)}\right) \end{aligned} \tag{9}$$

3.1. Center of gravity and moment of inertia

Movement of masses not only changes the CoG and moment of inertia (I) but also creates multiple derivative terms of the moment of inertia in equations. In order to calculate the effect of CoG displacement on the moment of inertia matrix and CoG, we consider a general displacement of the masses, where the displacement of longitudinal masses (m_1 and m_3) is χ and the displacement of lateral masses (m_2 and m_4) is Υ.

According to the Fig. 4, the position vector of the masses in the R_0 frame are:

$$r_1^0 = \begin{bmatrix} \chi & \frac{l}{2} & 0 \end{bmatrix}^T \tag{10}$$

$$r_2^0 = \begin{bmatrix} \frac{l}{2} & \Upsilon & 0 \end{bmatrix}^T \tag{11}$$

$$r_3^0 = \begin{bmatrix} \chi & -\frac{l}{2} & 0 \end{bmatrix}^T \tag{12}$$

$$r_4^0 = \begin{bmatrix} -\frac{l}{2} & \Upsilon & 0 \end{bmatrix}^T \tag{13}$$

where l is the square side length. Therefore, the position of the CoG in the R_0 frame will be:

$$\begin{aligned} r_c^0 &= \frac{m_b r_b^0 + \sum_{n=1}^4 m_n r_n^0}{m_b + \sum_{n=1}^4 m_n} \xrightarrow{r_b^0 = [0 \quad 0 \quad 0]^T} \\ \frac{\sum_{n=1}^4 m_n r_n^0}{M} &= \mu \cdot \begin{bmatrix} 2\chi & 2\Upsilon & 0 \end{bmatrix}^T \end{aligned} \tag{14}$$

where μ is the ratio of the mass of a single moving mass (which is equal to other moving masses) to overall mass (m_n/M). The position vector of the moving masses in the R_1 frame can be calculated as follows:

$$r_n^1 = r_n^0 - r_c^0 \tag{15}$$

So:

$$r_1^1 = \begin{bmatrix} \chi(1-2\mu) & \frac{l}{2} - 2\mu\Upsilon & 0 \end{bmatrix}^T \tag{16}$$

$$r_2^1 = \begin{bmatrix} \frac{l}{2} - 2\mu\chi & \Upsilon(1-2\mu) & 0 \end{bmatrix}^T \tag{17}$$

$$r_3^1 = \begin{bmatrix} \chi(1-2\mu) & -\left(\frac{l}{2} + 2\mu\Upsilon\right) & 0 \end{bmatrix}^T \tag{18}$$

$$r_4^1 = \begin{bmatrix} -\left(\frac{l}{2} + 2\mu\chi\right) & \Upsilon(1-2\mu) & 0 \end{bmatrix}^T \tag{19}$$

Simply the position vector of the body in the R_1 frame will be achieved:

$$r_b^1 = -r_c^0 = -\mu \cdot \begin{bmatrix} 2\chi & 2\Upsilon & 0 \end{bmatrix}^T \tag{20}$$

It is clear that the overall moment of inertia of the UAV is the summation of the moment of inertia of all components:

$$I_s^1 = I_b^1 + \sum_{n=1}^4 I_n^1 \tag{21}$$

We consider five components, one of them is the body without moving masses and four others are the moving masses. In order to calculate the moment of inertia of the UAV, we should calculate the moment of inertia of the body and four moving masses around the CoG. By using the Parallel Axis Theorem for a desired mass m we have [17]:

$$I_m^1 = \overline{I}_m + m_m\left(r_m^{1T} \cdot r_m^1 E_3 - r_m^1 \cdot r_m^{1T}\right) \tag{22}$$

The moment of inertia of the body around CoG is:

$$\begin{aligned} &I_b^1 = \overline{I}_b + m_b\left(r_b^{1T} \cdot r_b^1 E_3 - r_b^1 \cdot r_b^{1T}\right) = \\ &\overline{I}_b + m_b \begin{pmatrix} \mu^2 \begin{bmatrix} 2\chi & 2\Upsilon & 0 \end{bmatrix} \begin{bmatrix} 2\chi \\ 2\Upsilon \\ 0 \end{bmatrix} \begin{bmatrix} 1 & 0 & 0 \\ 0 & 1 & 0 \\ 0 & 0 & 1 \end{bmatrix} \\ -\mu^2 \begin{bmatrix} 2\chi \\ 2\Upsilon \\ 0 \end{bmatrix} \begin{bmatrix} 2\chi & 2\Upsilon & 0 \end{bmatrix} \end{pmatrix} = \\ &\overline{I}_b + \\ &\begin{bmatrix} 4m_b\mu^2\Upsilon^2 & -4m_b\mu^2\chi\Upsilon & 0 \\ -4m_b\mu^2\chi\Upsilon & 4m_b\mu^2\chi^2 & 0 \\ 0 & 0 & -4m_b\mu^2(\chi^2 + \Upsilon^2) \end{bmatrix} \end{aligned} \tag{23}$$

where $\bar{I}_b$ is the moment of inertia of the body (except the moving masses) around its center of gravity, and m_b is the mass of body without moving masses. The moment of inertia of the moving masses will be calculated in the same way, hence the overall moment of inertia of the system around the CoG will be:

$$I_s^1 = \bar{I}_b + 4\bar{I}_m + \begin{bmatrix} \sigma_{10}+\sigma_6+\sigma_5 \\ +\sigma_3-\sigma_8 & \sigma_1 & 0 \\ \sigma_1 & \sigma_9+\sigma_6+\sigma_4 \\ & +\sigma_2-\sigma_7 & 0 \\ 0 & 0 & ml^2+\sigma_{10}+\sigma_9 \\ & & +\sigma_5+\sigma_4+\sigma_3 \\ & & +\sigma_2-\sigma_8-\sigma_7 \end{bmatrix} \tag{24}$$

where:

$$\begin{aligned} &\sigma_2 = 4m_b\mu^2\chi^2 \quad \sigma_3 = 4m_b\mu^2\Upsilon^2 \quad \sigma_4 = 16m\mu^2\chi^2 \\ &\sigma_5 = 16m\mu^2\Upsilon^2 \quad \sigma_6 = \frac{ml^2}{2} \quad \sigma_7 = 8m\mu\Upsilon^2 \\ &\sigma_8 = 8m\mu\chi^2 \quad \sigma_9 = 2m\chi^2 \quad \sigma_{10} = 2m\Upsilon^2 \\ &\sigma_1 = -4\mu\chi\Upsilon(4m\mu - 2m + m_b\mu) \end{aligned} \tag{25}$$

Accordingly, the derivate of the moment of inertia is:

$$\dot{I}_s^1 = \begin{bmatrix} \dot{\sigma}_{10}+\dot{\sigma}_6+\dot{\sigma}_5 \\ +\dot{\sigma}_3-\dot{\sigma}_8 & \dot{\sigma}_1 & 0 \\ \dot{\sigma}_1 & \dot{\sigma}_9+\dot{\sigma}_6+\dot{\sigma}_4 \\ & +\dot{\sigma}_2-\dot{\sigma}_7 & 0 \\ 0 & 0 & \dot{\sigma}_{10}+\dot{\sigma}_9+\dot{\sigma}_5 \\ & & +\dot{\sigma}_4+\dot{\sigma}_3 \\ & & +\dot{\sigma}_2-\dot{\sigma}_8-\dot{\sigma}_7 \end{bmatrix} \tag{26}$$

where:

$$\begin{aligned} &\dot{\sigma}_2 = 8m_b\mu^2\chi\dot{\chi} \quad \dot{\sigma}_3 = 8m_b\mu^2\Upsilon\dot{\Upsilon} \quad \dot{\sigma}_4 = 32m\mu^2\chi\dot{\chi} \\ &\dot{\sigma}_5 = 32m\mu^2\Upsilon\dot{\Upsilon} \quad \dot{\sigma}_6 = 0 \quad \dot{\sigma}_7 = 16m\mu\Upsilon\dot{\Upsilon} \\ &\dot{\sigma}_8 = 16m\mu\chi\dot{\chi} \quad \dot{\sigma}_9 = 4m\chi\dot{\chi} \quad \dot{\sigma}_{10} = 4m\Upsilon\dot{\Upsilon} \\ &\dot{\sigma}_1 = -4\mu\dot{\chi}\Upsilon(4m\mu - 2m + m_b\mu) \\ &\qquad - 4\mu\chi\dot{\Upsilon}(4m\mu - 2m + m_b\mu) \end{aligned} \tag{27}$$

3.2. Dynamic equations

The R_0 is a rotating frame, so the derivative of the vector r_0 in the R_i frame will be [17]:

$$\frac{d^{\{i\}}}{dt}\left(r_0^0\right) = \dot{r}_0^0 + \omega \times r_0^0 \tag{28}$$

where $\frac{d^{\{i\}}}{dt}$ denotes the time derivative of a vector in the rotating frame (R_0) w.r.t the inertial frame (R_i) and ω is the angular velocity of the rotating frame (R_0) w.r.t the inertial frame.

Thus, the velocity of the CoG in the R_i frame is:

$$v_c^i = v_b^i + v_c^0 + \omega \times r_c^0 \tag{29}$$

where v_c^0 is the time derivative of the r_c^0:

$$v_c^0 = \frac{\sum_{n=1}^4 m_n \dot{r}_n^0}{M} \tag{30}$$

Similarly, for the nth mass:

$$v_n^i = v_b^i + v_n^0 + \omega \times r_n^0 \tag{31}$$

The linear momentum of the nth mass is:

$$L_n^0 = m_n \cdot v_n^0 \tag{32}$$

Linear momentum of the overall system in the inertial frame is:

$$L_s^i = L_b^i + \sum_{n=1}^4 L_n^i \tag{33}$$

Using Eq. (14), Eq. (31), Eq. (32) one can write:

$$\begin{aligned} L_s^i &= M\left(v_b^i + \omega \times r_c^0\right) + \sum_{n=1}^4 m_n v_n^0 \\ &= M\left(v_b^i + \omega \times r_c^0\right) + \sum_{n=1}^4 L_n^0 \end{aligned} \tag{34}$$

By using the second law of Newton we have:

$$\begin{aligned} \frac{d^{\{i\}}}{dt} v_b^i = \frac{1}{M}\left(\sum_{j=1}^2 F_{rj} + F_g + F_d - \frac{d^i}{dt}\left(\sum_{n=1}^4 L_n^0\right)\right) \\ - \frac{d^i}{dt}\left(\omega \times r_c^0\right) \end{aligned} \tag{35}$$

where F_{rj} is the propellant force of the jth rotor, which is calculated by:

$$F_{rj} = T_b^v\left(b\Omega_j^2\hat{k}\right) \tag{36}$$

where b is the rotor constant, Ω is the angular velocity of the rotor and $\hat{k}$ is the unit vector of the Z-axis in the body frame.

Also, the weight force is:

$$F_g = -Mg\hat{K} \tag{37}$$

where $\hat{K}$ is the unit vector of the Z-axis in the inertial frame.

And F_d is external forces in the inertial frame.

Angular momentum of the system in the R_1 frame equals to the sum of angular momentum of all components:

$$H_s^1 = H_b^1 + \sum_{n=1}^4 H_n^1 \tag{38}$$

where H_b is angular momentum of the body and H_n is the angular momentum of nth moving mass, we have:

$$H_s^1 = I_s^1\omega + \sum_{n=1}^4 r_n^1 \times L_n^0 \tag{39}$$

Using the second law of Newton for rotation, yields:

$$\frac{d^{\{i\}}}{dt}\left(I_s^1\omega + \sum_{n=1}^4 r_n^1 \times L_n^0\right) = \sum_{j=1}^2 \left(M_{tj} + M_{rj}\right) + M_g + M_d \tag{40}$$

where M_{tj} is the torque of the jth rotor's thrust and M_{rj} is the reaction torque of the jth rotor:

$$M_{tj} = -r_c^0 \times F_{rj} \tag{41}$$

$$M_{rj} = (-1)^{j+1} d\Omega^2\hat{k} \tag{42}$$

in where d is rotor constant, also M_g is the torque of the weight force:

$$M_g = r_b^1 \times \left(-m_b g\hat{K}\right) + \sum_{n=1}^4 r_n^1 \times \left(-m_n g\hat{K}\right) \tag{43}$$

and M_d is external momentums in body frame.

As we are calculating the angular momentum w.r.t CoG it is clear that M_g =0.

3.3. Expanding the translational equations

The left-hand side of the (35) is:

$$\frac{d^{\{i\}}}{dt} v_b^i = a_b^i = \begin{bmatrix} \ddot{x} & \ddot{y} & \ddot{z} \end{bmatrix}^T \tag{44}$$

for the term $\frac{d^i}{dt}(\sum_{n=1}^{4} L_n^0)$ we have:

$$\begin{aligned} \frac{d^{\{i\}}}{dt}\left(\sum_{n=1}^{4} L_n^0\right) &= \sum_{n=1}^{4} \dot{L}_n^0 + \omega \times L_n^0 \\ &\xrightarrow{L_n^0 = m \cdot v_n^0} \sum_{n=1}^{4} m \cdot \dot{v}_n^0 + \omega \times m \cdot v_n^0 \end{aligned} \tag{45}$$

where $\times$ is the vector cross operator, thus:

$$\begin{aligned} \frac{d^{\{i\}}}{dt}\left(\sum_{n=1}^{4} L_n^0\right) &= m \begin{bmatrix} 2\ddot{\chi} \\ 2\ddot{\Upsilon} \\ 0 \end{bmatrix} + m \begin{bmatrix} -2\omega_z \dot{\Upsilon} \\ 2\omega_z \dot{\chi} \\ 2\omega_x \dot{\Upsilon} - 2\omega_y \dot{\chi} \end{bmatrix} \\ &= m \begin{bmatrix} 2\ddot{\chi} - 2\omega_z \dot{\Upsilon} \\ 2\ddot{\Upsilon} + 2\omega_z \dot{\chi} \\ 2\omega_x \dot{\Upsilon} - 2\omega_y \dot{\chi} \end{bmatrix} \end{aligned} \tag{46}$$

Consequently, the term $\frac{d^i}{dt}(\omega \times r_c^0)$ will be:

$$\begin{aligned} \frac{d^{\{i\}}}{dt}\left(\omega \times r_c^0\right) &= \frac{d^i}{dt}\left(\begin{bmatrix} \omega_x \\ \omega_y \\ \omega_z \end{bmatrix} \times \begin{bmatrix} 2\mu\chi \\ 2\mu\Upsilon \\ 0 \end{bmatrix}\right) \\ &= \frac{d^{\{i\}}}{dt}\left(\begin{bmatrix} -2\omega_z \mu\Upsilon \\ 2\omega_z \mu\chi \\ 2\omega_x \mu\Upsilon - 2\omega_y \mu\chi \end{bmatrix}\right) \\ &= \begin{bmatrix} -2\dot{\omega}_z \mu\Upsilon - 2\omega_z \mu\dot{\Upsilon} \\ 2\dot{\omega}_z \mu\chi + 2\omega_z \mu\dot{\chi} \\ 2\dot{\omega}_x \mu\Upsilon - 2\dot{\omega}_y \mu\chi + 2\omega_x \mu\dot{\Upsilon} - 2\omega_y \mu\dot{\chi} \end{bmatrix} \\ &\quad + \begin{bmatrix} 2\mu\Upsilon\omega_x\omega_y - 2\mu\chi\omega_y^2 - 2\mu\chi\omega_z^2 \\ -2\mu\Upsilon\omega_y^2 - 2\mu\Upsilon\omega_x^2 - 2\mu\chi\omega_x\omega_y \\ 2\mu\Upsilon\omega_y\omega_z + 2\mu\chi\omega_x\omega_z \end{bmatrix} \end{aligned} \tag{47}$$

As ω is expressed in the inertial frame, using Eq. (1) the nonlinear translational equations are simplified to:

$$\begin{aligned} \ddot{x} &= \frac{b}{M}\left(\Omega_1^2 + \Omega_2^2\right)(c(\varphi)s(\theta)c(\psi) + s(\varphi)s(\psi)) \\ &\quad - \mu(2\ddot{\chi} - 2r\dot{\Upsilon}) - (-2\dot{r}\mu\Upsilon - 2r\mu\dot{\Upsilon}) \\ &\quad - \left(2\mu\Upsilon pq - 2\mu\chi q^2 - 2\mu\chi r^2\right) + F_{d,x} \\ \ddot{y} &= \frac{b}{M}\left(\Omega_1^2 + \Omega_2^2\right)(c(\varphi)s(\theta)s(\psi) - s(\varphi)c(\psi)) - \mu(2\ddot{\Upsilon} + 2r\dot{\chi}) \\ &\quad - (2\dot{r}\mu\chi + 2r\mu\dot{\chi}) - \left(-2\mu\Upsilon q^2 - 2\mu\Upsilon p^2 - 2\mu\chi pq\right) \\ &\quad + F_{d,y} \\ \ddot{z} &= \frac{b}{M}\left(\Omega_1^2 + \Omega_2^2\right)(c(\varphi)c(\theta)) - g - \mu(2p\dot{\Upsilon} - 2q\dot{\chi}) \\ &\quad - (2\dot{p}\mu\Upsilon - 2\dot{q}\mu\chi + 2p\mu\dot{\Upsilon} - 2q\mu\dot{\chi}) - (2\mu\Upsilon qr + 2\mu\chi pr) \\ &\quad + F_{d,z} \end{aligned} \tag{48}$$

where $F_{d,x}$, $F_{d,y}$ and $F_{d,z}$ are the elements of the external forces in x, y and z directions.

Note that the air drag is neglected in the abovementioned equations.

3.4. Expanding the rotational equations

The left-hand side of the (40) is:

$$\begin{aligned} &\frac{d^{\{i\}}}{dt}\left(I_s^1 \omega + \sum_{n=1}^{4} r_n^1 \times L_n^0\right) = \\ &\dot{I}_s^1 \omega + I_s^1 \dot{\omega} + \omega \times \left(I_s^1 \omega\right) + \omega \times \left(\sum_{n=1}^{4} r_n^1 \times L_n^0\right) \\ &\quad + \sum_{n=1}^{4} \dot{r}_n^1 \times L_n^0 + \sum_{n=1}^{4} r_n^1 \times \dot{L}_n^0 \end{aligned} \tag{49}$$

where the terms $\dot{I}_s^1$ and I_s^1 are calculated previously in (24), (26), and the term $\omega \times \left(I_s^1 \omega\right)$ is:

$$\begin{aligned} &\omega \times \left(I_s^1 \omega\right) = \\ &\begin{bmatrix} \omega_y \left(\begin{matrix} I_{zx}\omega_x + \\ I_{zy}\omega_y + I_{zz}\omega_z \end{matrix}\right) - \omega_z \left(\begin{matrix} I_{yx}\omega_x + \\ I_{yy}\omega_y + I_{yz}\omega_z \end{matrix}\right) \\ \omega_z \left(\begin{matrix} I_{xx}\omega_x + \\ I_{xy}\omega_y + I_{xz}\omega_z \end{matrix}\right) - \omega_x \left(\begin{matrix} I_{zx}\omega_x + \\ I_{zy}\omega_y + I_{zz}\omega_z \end{matrix}\right) \\ \omega_x \left(\begin{matrix} I_{yx}\omega_x + \\ I_{yy}\omega_y + I_{yz}\omega_z \end{matrix}\right) - \omega_y \left(\begin{matrix} I_{xx}\omega_x + \\ I_{xy}\omega_y + I_{xz}\omega_z \end{matrix}\right) \end{bmatrix} \end{aligned} \tag{50}$$

Using Eq. (16), Eq. (17), Eq. (18), Eq. (19), Eq. (32) it can be obtained:

$$\sum_{n=1}^{4} r_n^1 \times L_n^0 = \begin{bmatrix} 0 \\ 0 \\ 4m\mu\Upsilon\dot{\chi} - 4m\mu\chi\dot{\Upsilon} \end{bmatrix} \tag{51}$$

therefore $\omega \times \left(\sum_{n=1}^{4} r_n^1 \times L_n^0\right)$ can be computed as follows:

$$\omega \times \sum_{n=1}^{4} r_n^1 \times L_n^0 = \begin{bmatrix} \omega_y \left(4m\mu\Upsilon\dot{\chi} - 4m\mu\chi\dot{\Upsilon}\right) \\ \omega_x \left(4m\mu\Upsilon\dot{\chi} - 4m\mu\chi\dot{\Upsilon}\right) \\ 0 \end{bmatrix} \tag{52}$$

Similarly, the term $\sum_{n=1}^{4} r_n^1 \times \dot{L}_n^0$ will be:

$$\sum_{n=1}^{4} r_n^1 \times \dot{L}_n^0 = \begin{bmatrix} 0 \\ 0 \\ 4m\mu\Upsilon\ddot{\chi} - 4m\mu\chi\ddot{\Upsilon} \end{bmatrix} \tag{53}$$

The term $\sum_{n=1}^{4} \dot{r}_n^1 \times L_n^0$ is zero:

$$\begin{aligned} \sum_{n=1}^{4} \dot{r}_n^1 \times L_n^0 &= \begin{bmatrix} 0 \\ 0 \\ 2m\mu\dot{\chi}\dot{\Upsilon} \end{bmatrix} + \begin{bmatrix} 0 \\ 0 \\ -2m\mu\dot{\chi}\dot{\Upsilon} \end{bmatrix} \\ &\quad + \begin{bmatrix} 0 \\ 0 \\ 2m\mu\dot{\chi}\dot{\Upsilon} \end{bmatrix} + \begin{bmatrix} 0 \\ 0 \\ -2m\mu\dot{\chi}\dot{\Upsilon} \end{bmatrix} = \begin{bmatrix} 0 \\ 0 \\ 0 \end{bmatrix} \end{aligned} \tag{54}$$

In order to calculate the term $\sum_{j=1}^{2}(M_{tj} + M_{dj})$ we should replace (14), (36), (41), (42) in (40):

$$\begin{aligned} M_{tj} &= -r_c^0 \times F_{rj} = \begin{bmatrix} -2\mu\chi \\ -2\mu\Upsilon \\ 0 \end{bmatrix} \times \begin{bmatrix} 0 \\ 0 \\ b\left(\Omega_1^2 + \Omega_2^2\right) \end{bmatrix} \\ &= \begin{bmatrix} -2b\mu\Upsilon\left(\Omega_1^2 + \Omega_2^2\right) \\ 2b\mu\chi\left(\Omega_1^2 + \Omega_2^2\right) \\ 0 \end{bmatrix} \end{aligned} \tag{55}$$

$$M_{dj} = (-1)^{j+1} d\Omega^2 \hat{k} = \begin{bmatrix} 0 \\ 0 \\ d\left(\Omega_1^2 - \Omega_2^2\right) \end{bmatrix} \tag{56}$$

Finally, the nonlinear rotational equations can be derived:

$$\begin{aligned}\dot{p} =& -\frac{I_{xy}\dot{q}}{I_{xx}} - \frac{I_{xz}\dot{r}}{I_{xx}} - \frac{\dot{I}_{xx}p}{I_{xx}} - \frac{\dot{I}_{xy}q}{I_{xx}} - \frac{\dot{I}_{xz}r}{I_{xx}} \\ & - \frac{q\left(I_{zx}p + I_{zy}q + I_{zz}r\right)}{I_{xx}} + \frac{r\left(I_{yx}p + I_{yy}q + I_{yz}r\right)}{I_{xx}} \\ & - \frac{q\left(4m\mu\Upsilon\dot{\chi} - 4m\mu\chi\dot{\Upsilon}\right)}{I_{xx}} - \frac{2b\mu\Upsilon\left(\Omega_1^2 + \Omega_2^2\right)}{I_{xx}} \\ & + M_{d,x} \\ \dot{q} =& -\frac{I_{yx}\dot{p}}{I_{yy}} - \frac{I_{yz}\dot{r}}{I_{yy}} - \frac{\dot{I}_{yx}p}{I_{yy}} - \frac{\dot{I}_{yy}q}{I_{yy}} - \frac{\dot{I}_{yz}r}{I_{yy}} \\ & - \frac{r\left(I_{xx}p + I_{xy}q + I_{xz}r\right)}{I_{yy}} + \frac{p\left(I_{zx}p + I_{zy}q + I_{zz}r\right)}{I_{yy}} \\ & - \frac{p\left(4m\mu\Upsilon\dot{\chi} - 4m\mu\chi\dot{\Upsilon}\right)}{I_{yy}} + \frac{2b\mu\chi\left(\Omega_1^2 + \Omega_2^2\right)}{I_{yy}} \\ & + M_{d,y} \\ \dot{r} =& -\frac{I_{zx}\dot{p}}{I_{zz}} - \frac{I_{zy}\dot{q}}{I_{zz}} - \frac{\dot{I}_{zx}p}{I_{zz}} - \frac{\dot{I}_{zy}q}{I_{zz}} - \frac{\dot{I}_{zz}r}{I_{zz}} \\ & - \frac{p\left(I_{yx}p + I_{yy}q + I_{yz}r\right)}{I_{zz}} + \frac{q\left(I_{xx}p + I_{xy}q + I_{xz}r\right)}{I_{zz}} \\ & - \frac{4m\mu\Upsilon\ddot{\chi}}{I_{zz}} - \frac{4m\mu\chi\ddot{\Upsilon}}{I_{zz}} + \frac{d\left(\Omega_1^2 - \Omega_2^2\right)}{I_{zz}} + M_{d,z} \end{aligned} \tag{57}$$

Where $M_{d,x}$, $M_{d,y}$ and $M_{d,z}$ are the elements of external momentums in x, y and z direction of the body frame.

4. 3DOF planar motion

In this section, we consider the motion of the UAV in the YZ plane. Firstly, multiple simplifying assumptions should be considered:

- The effect of displacement of the moving masses on I is neglectable, hence I is considered to be a constant diagonal matrix.
- The terms m, μ, χ, and Υ are pretty small, thus it is reasonable to consider that the translational and rotational motion of the UAV is only affected by the propellants forces and torques, and other forces (which are created due to the displacement of the moving masses) can be neglected.
- The angels θ and ψ are considered to be zero.
- Displacement of the masses in the direction of y axis (Υ) is zero.
- External forces and momentums are zero.

It should be noted that the simplifications and approximations considered above, can be regarded as uncertainties. Using the above considerations, the simplified nonlinear 3DOF equations of motion can be written as follows:

$$\ddot{y} = \frac{b}{M}\left(\Omega_1^2 + \Omega_2^2\right)(-\sin(\varphi)) \tag{58}$$

$$\ddot{z} = \frac{b}{M}\left(\Omega_1^2 + \Omega_2^2\right)(\cos(\varphi)) - g \tag{59}$$

$$\ddot{\varphi} = -\frac{2b\mu\Upsilon\left(\Omega_1^2 + \Omega_2^2\right)}{I_{xx}} \tag{60}$$

4.1. Linearization

Considering u_1 as:

$$u_1 = b\left(\Omega_1^2 + \Omega_2^2\right) \tag{61}$$

and u_2 as:

$$u_2 = \Upsilon \tag{62}$$

by using Eq. (62) and Eq. (63), the Eq. (58), Eq. (59) and Eq. (60) become:

$$\ddot{y} = f_1(\varphi.u_1.u_2) = -\frac{\sin(\varphi)}{M}u_1 \tag{63}$$

$$\ddot{z} = f_2(\varphi.u_1.u_2) = -g + \frac{\cos(\varphi)}{M}u_1 \tag{64}$$

$$\ddot{\varphi} = f_3(\varphi.u_1.u_2) = -\frac{2\mu}{I_{xx}}u_1u_2 \tag{65}$$

The equilibrium point considers at the hover condition where:

$$u_{1,e} = Mg, \quad u_{2,e} = 0, \quad \varphi_e = 0$$

So the linear functions at the equilibrium point can be calculated as follows [19]:

$$\begin{aligned} F_1 =& \left.\frac{\partial f_1}{\partial u_1}\right|_{u_{1.e}.\varphi_e.u_{2.e}}(u_1 - u_{1.e}) \\ & + \left.\frac{\partial f_1}{\partial u_2}\right|_{u_{1.e}.\varphi_e.u_{2.e}}(u_2 - u_{2.e}) \\ & + \left.\frac{\partial f_1}{\partial \varphi}\right|_{u_{1.e}.\varphi_e.u_{2.e}}(\varphi - \varphi_e) \\ =& -g\varphi \end{aligned} \tag{66}$$

$$\begin{aligned} F_2 =& \left.\frac{\partial f_2}{\partial u_1}\right|_{u_{1.e}.\varphi_e.u_{2.e}}(u_1 - u_{1.e}) \\ & + \left.\frac{\partial f_2}{\partial u_2}\right|_{u_{1.e}.\varphi_e.u_{2.e}}(u_2 - u_{2.e}) \\ & + \left.\frac{\partial f_2}{\partial \varphi}\right|_{u_{1.e}.\varphi_e.u_{2.e}}(\varphi - \varphi_0) \\ =& \frac{1}{M}u_1 - g \end{aligned} \tag{67}$$

$$\begin{aligned} F_3 =& \left.\frac{\partial f_3}{\partial u_1}\right|_{u_{1.e}.\varphi_e.u_{2.e}}(u_1 - u_{1.e}) \\ & + \left.\frac{\partial f_3}{\partial u_2}\right|_{u_{1.e}.\varphi_e.u_{2.e}}(u_2 - u_{2.e}) \\ & + \left.\frac{\partial f_3}{\partial \varphi}\right|_{u_{1.e}.\varphi_e.u_{2.e}}(\varphi - \varphi_e) \\ =& -\frac{2\mu}{I_{xx}}Mgu_2 \end{aligned} \tag{68}$$

then the linear model of the system under hover conditions can be summarized as:

$$\begin{cases} \ddot{y} = -g\varphi \\ \ddot{z} = -g + \dfrac{1}{M}u_1 \\ \ddot{\varphi} = -\dfrac{2\mu}{I_{xx}}Mgu_2 \end{cases} \tag{69}$$

Therefore, the state-space model becomes:

$$\begin{bmatrix} \dot{y} \\ \dot{z} \\ \dot{\varphi} \\ \ddot{y} \\ \ddot{z} \\ \ddot{\varphi} \end{bmatrix} = \begin{bmatrix} 0 & 0 & 0 & 1 & 0 & 0 \\ 0 & 0 & 0 & 0 & 1 & 0 \\ 0 & 0 & 0 & 0 & 0 & 1 \\ 0 & 0 & -g & 0 & 0 & 0 \\ 0 & 0 & 0 & 0 & 0 & 0 \\ 0 & 0 & 0 & 0 & 0 & 0 \end{bmatrix} \begin{bmatrix} y \\ z \\ \varphi \\ \dot{y} \\ \dot{z} \\ \dot{\varphi} \end{bmatrix} + \begin{bmatrix} 0 & 0 \\ 0 & 0 \\ 0 & 0 \\ 0 & 0 \\ \frac{1}{M} & 0 \\ 0 & \frac{-2\mu}{I_{xx}} Mg \end{bmatrix} \begin{bmatrix} u_1 \\ u_2 \end{bmatrix} \tag{70}$$

in which the state vector is defined as follows:

$$X = \begin{bmatrix} y & z & \varphi & \dot{y} & \dot{z} & \dot{\varphi} \end{bmatrix}^T \tag{71}$$

Considering Y as:

$$Y = \begin{bmatrix} y & z \end{bmatrix}^T \tag{72}$$

the C and D matrixes will be:

$$C = \begin{bmatrix} 1 & 0 & 0 & 0 & 0 & 0 \\ 0 & 1 & 0 & 0 & 0 & 0 \end{bmatrix} \tag{73}$$

$$D = \begin{bmatrix} 0 & 0 \\ 0 & 0 \end{bmatrix} \tag{74}$$

4.2. Stability check

Considering A, B, C, D matrixes as described previously, the characteristic equation of y channel will be of 4th order and z channel will be of 2nd order, the system has 4 poles in the origin, so the system is marginally stable.

4.3. Controllability and observability check

In order to design an LQR controller, it is necessary to check the controllability of the system; the controllability matrix of the system defines as:

$$M = \begin{bmatrix} B & AB & A^2B & \dots & A^{n-1}B \end{bmatrix} \tag{75}$$

The system is fully controllable if and only if the M has full rank. Also, the Observability Matrix defines as:

$$O = \begin{bmatrix} C & CA & CA^2 & \dots & CA^{n-1} \end{bmatrix}^T \tag{76}$$

Similarly, the system is completely observable if and only if the O has full rank [18].

Using MATLAB or any other mathematical software like Maple and Octave, it can be easily shown that the ranks of both M and O matrices are 6 and the system is fully controllable and observable.

5. Linear quadratic regulator

For a state-regulator system with infinite time interval and cost function as follows:

$$J = \frac{1}{2} \int_0^\infty \left[x'(t)\, Q\, x(t) + u'(t)\, R u(t) \right] dt \tag{77}$$

The state feedback gain, K, can be calculated from:

$$K = -R^{-1} B^T \overline{P} \tag{78}$$

where $\overline{P}$ is the solution of algebraic Riccati equation [20]:

$$\overline{P}A + A^T\overline{P} + Q - \overline{P}BR^{-1}B^T\overline{P} = 0 \tag{79}$$

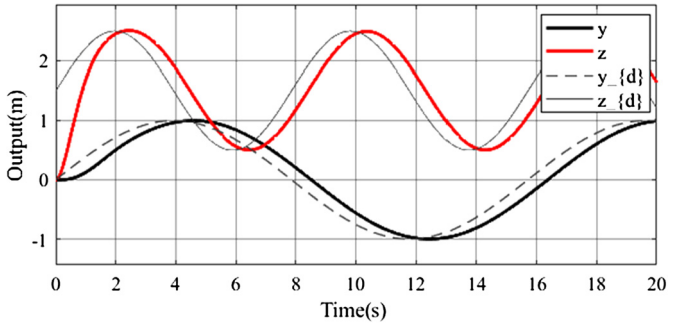

Fig. 5. Response of the system to the 8 shape input.

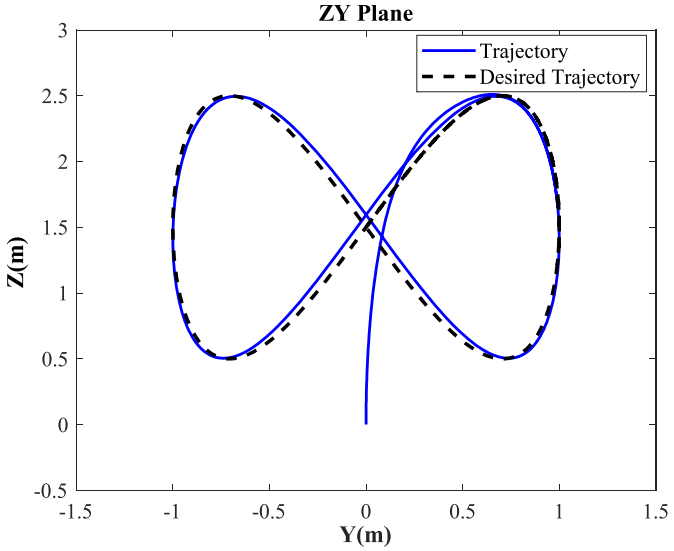

Fig. 6. System trajectory and desired trajectory.

6. LQR controller for tracking

In order to investigate the maneuverability of the system, it is common to consider a fast 8-shape trajectory, as a tracking mission for the system.

With regard to the tracking problem, we can define new states as follows:

$$X' = X_d - X = \begin{bmatrix} e_y \\ e_z \\ e_\varphi \\ e_{\dot{y}} \\ e_{\dot{z}} \\ e_{\dot{\varphi}} \end{bmatrix} = \begin{bmatrix} y_d - y \\ z_d - z \\ \varphi_d - \varphi \\ \dot{y}_d - \dot{y} \\ \dot{z}_d - \dot{z} \\ \dot{\varphi}_d - \dot{\varphi} \end{bmatrix} \tag{80}$$

where X_d is the desired trajectory in the state space which is defined as:

$$y_d = \sin(0.4t) \tag{81}$$

$$z_d = \sin(0.8t) + 1.5 \tag{82}$$

The above defined trajectory is a fast-enough and challenging trajectory which can determine the maneuverability of the system. Considering some adjustments in Q and R matrices by trial and error in order to satisfy control constraints in tracking above-defined trajectory, and initial condition in the origin, the response of the system for the 8-shape trajectory is depicted in Fig. 5.

In this case, the trajectory of the system in the ZY plane is described in Fig. 6.

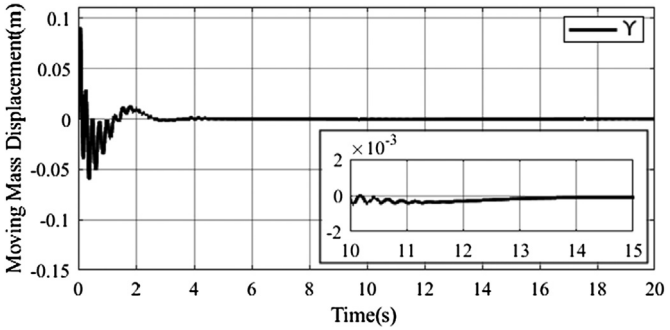

Fig. 7. Displacement of the moving masses.

Table 1
Different uncertainties considered in simulations.

Condition	Parameter	Amount
Cond 1	Uncertainty in M_b	10%
Cond 2	Uncertainty in m	20%
Cond 3	Propellant force angle	5°
Cond 4	Propellant efficiency	90%

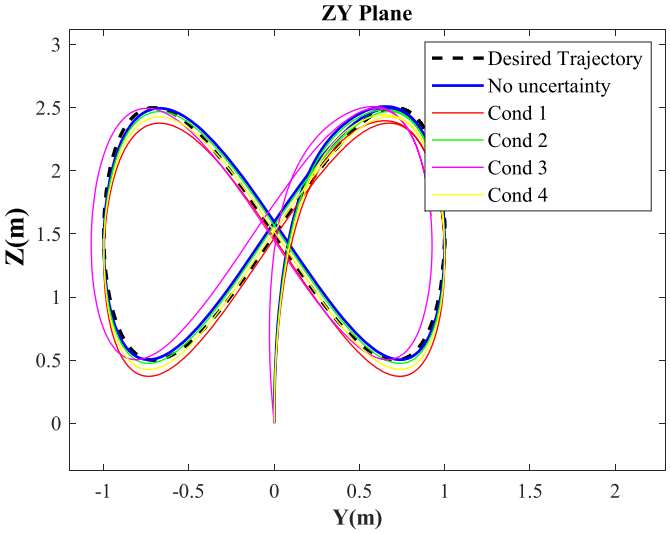

Fig. 8. System trajectory for different conditions. (For interpretation of the colors in the figure(s), the reader is referred to the web version of this article.)

The displacement of the moving mass, is under 0.25 m which is achieved by adjusting the R matrix by trail and error (see Fig. 7).

Even by considering uncertainties in model, controller performance and system maneuverability will be acceptable for this specific nominal trajectory, to show this, we consider four different conditions with some desired uncertainties as described in Table 1 (see also Fig. 8).

Displacement of the moving masses in the different conditions is shown in Fig. 9.

As the results show, the system has acceptable maneuverability even with control limits in the roll channel and different uncertainties. The performance of the system in the pitch channel can be estimated to be the same as the roll channel, so it can be concluded that the system has good enough maneuverability and convincing performance. Even though this concept is more complicated than a quadrotor or some other UAVs in mathematical model, it has some benefits which make it appropriate for common applications, e.g. aerial post and delivery, aerial taxi, forestry, agriculture, multimedia, patrolling, traffic control etc. as well as applications which needs higher maneuverability like military applications and FPV racing. Furthermore, using this kind of concept

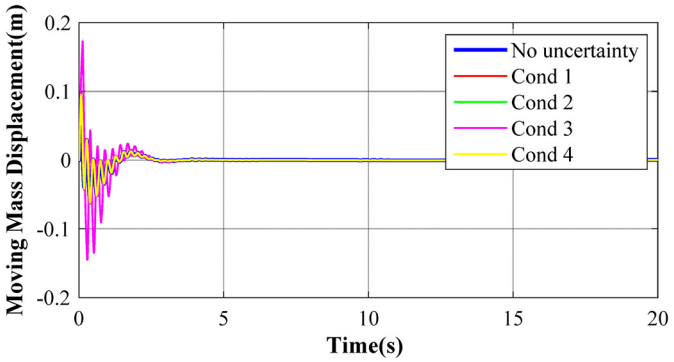

Fig. 9. Displacement of the moving masses in different conditions.

makes it possible to reform the mass imbalances and tune the overall mass distribution, in order to keep the CoG at the center of surface (where the propellant force is acting) and achieve stability.

It should be considered that the maneuverability of the system can be improved by increasing the mass of the moving masses. However, it may increase the cost and energy consumption, and specifically, decrease payload capacity. An optimization problem can be solved to determine the optimum mass of the moving masses.

7. Conclusion

In this paper, we have presented a novel concept of a bi-rotor VTOL unmanned aerial vehicle which is controlled based on Moving Mass Control. MMC mechanism is used in our concept to shift the CoG of the UAV to control the attitude. we derived a nonlinear 6DOF mathematical model of this kind of UAV and simplified this model to a 3DOF planar motion model. Finally, LQR control was implemented to evaluate the performance and maneuverability of the concept considering various uncertainties. The results indicate that this idea can provide good enough maneuverability to track a fast 8-shape trajectory, which is one of the most difficult tracking missions.

Declaration of competing interest

The authors declare that they have no known competing financial interests or personal relationships that could have appeared to influence the work reported in this paper.

References

[1] H. Shakhatreh, et al., Unmanned aerial vehicles (UAVs): a survey on civil applications and key research challenges, IEEE Access 7 (2019) 48572–48634, https://doi.org/10.1109/ACCESS.2019.2909530.
[2] K. Kanistras, G. Martins, M.J. Rutherford, K.P. Valavanis, Survey of unmanned aerial vehicles (UAVs) for traffic monitoring, in: Handbook of Unmanned Aerial Vehicles, Springer, Dordrecht, Netherlands, 2015, pp. 2643–2666.
[3] J. Everaerts, The use of unmanned aerial vehicles (UAVs) for remote sensing and mapping, Int. Arch. Photogramm. Remote Sens. Spat. Inf. Sci. 37 (2008) 1187–1192.
[4] Julian Tan Kok Ping, Ang Eng Ling, Tan Jun Quan, Chua Yea Dat, Generic unmanned aerial vehicle (UAV) for civilian application-a feasibility assessment and market survey on civilian application for aerial imaging, in: 2012 IEEE Conference on Sustainable Utilization and Development in Engineering and Technology (STUDENT), Oct. 2012, pp. 289–294.
[5] M. Hassanalian, A. Abdelkefi, Classifications, applications, and design challenges of drones: a review, Prog. Aerosp. Sci. 91 (May 2017) 99–131, https://doi.org/10.1016/j.paerosci.2017.04.003.
[6] S. Gupte, Paul Infant Teenu Mohandas, J.M. Conrad, A survey of quadrotor unmanned aerial vehicles, in: 2012 Proceedings of IEEE Southeastcon, Mar. 2012, pp. 1–6.

[7] A.S. Saeed, A.B. Younes, C. Cai, G. Cai, A survey of hybrid Unmanned Aerial Vehicles, Prog. Aerosp. Sci. 98 (2018) 91–105, https://doi.org/10.1016/j.paerosci.2018.03.007.
[8] J. Li, C. Gao, C. Li, W. Jing, A survey on moving mass control technology, Aerosp. Sci. Technol. 82–83 (September) (2018) 594–606, https://doi.org/10.1016/j.ast.2018.09.033.
[9] G. Changsheng, J. Wuxing, W. Pengxin, Research on application of single moving mass in the reentry warhead maneuver, Aerosp. Sci. Technol. 30 (1) (2013) 108–118.
[10] D. Kaixu, Z. Jun, Z. Min, Z. Bin, Roll control for single moving-mass actuated fixed-trim reentry vehicle considering full state constraints, Aerosp. Sci. Technol. 94 (2019).
[11] A. Mohammadi, M. Tayefi, K. Hamed, Rate regulation of a suborbital reentry payload by moving-mass actuators, Proc. Inst. Mech. Eng. Part G J. Aerosp. Eng. 227 (1) (2013) 80–92.
[12] G. Changsheng, L. Jianqing, F. Yidi, J. Wuxing, Immersion and invariance-based control of novel moving-mass flight vehicles, Aerosp. Sci. Technol. 74 (2018) 63–71.
[13] J. Wu-xing, L. Rui-kang, C. Gao, Roll control system design for moving mass re-entry vehicle based on optimal control, J. Astronaut. (2009).
[14] C. Bermes, S. Leutenegger, S. Bouabdallah, D. Schafroth, R. Siegwart, New design of the steering mechanism for a mini coaxial helicopter, 2008 IEEE/RSJ Int. Conf. Intell. Robot. Syst. IROS (2008) 1236–1241, https://doi.org/10.1109/IROS.2008.4650769.
[15] P.K. Yadav, K. Kalirajan, Dynamic model of a MAV with COG shifting mechanism, IFAC Proc. Vol. 3 (1) (2014) 380–385, https://doi.org/10.3182/20140313-3-IN-3024.00028.
[16] T. Haus, M. Orsag, S. Bogdan, Mathematical modelling and control of an unmanned aerial vehicle with moving mass control concept, J. Intell. Robot. Syst. Theory Appl. 88 (2–4) (2017) 219–246, https://doi.org/10.1007/s10846-017-0545-2.
[17] A. Frank D'Souza, Advanced Dynamics Modeling and Analysis, Prentice Hall, Inc., 2011.
[18] F. Sabatino, Quadrotor control: modeling, nonlinear control design, and simulation, Thesis, 2015.
[19] Francesco Sabatino, Quadrotor Control: Modeling, Nonlinear Control Design, and Simulation, KTH Royal Institute of Technology, 2015.
[20] D. Subbaram Naidu, Optimal Control Systems, CRC Press, 2002.